Materials Science Research International, Vol.6, No.4 pp.237-242 (2000)

General paper

X-Ray Stress Measurement for <110>-Oriented TiC Films

Shouichi EJIRI*, Juwen HE**, Toshihiko SASAKI*** and Yukio HIROSE***

*Seisen Jogakuin College, 2-120-8 Uwano, Nagano 381-0085, Japan

**Graduate student of Kanazawa University, Kakuma-machi, Kanazawa 920-1192, Japan

***Department of Materials Science, Kanazawa University, Kakuma-machi, Kanazawa 920-1192, Japan

Abstract: In this study, we investigate the residual stress of titanium carbide films with the X-ray diffraction method. It is difficult to determine the stress by conventional X-ray stress measurement, i.e., the $\sin^2\psi$ technique, because the $\sin^2\psi$ technique requires macroscopic isotropy from the specimen but the <110> orientation is observed for our evaporated TiC films by chemical vapor deposition. Therefore, in this paper, the X-ray stress measurement for <110>-oriented films was formulated by introducing the weighted average method. The formulation showed that the relation between the stress of the specimen and the strain measured by X-ray diffraction depended on the measured diffraction planes. Then, a stress calculation was performed and discussed based on the loading experiments.

Key words: *X-ray stress measurement, Titanium carbide films, Fiber texture, Residual stress, CVD*

1. INTRODUCTION

Recently, ceramic coating has become necessary as a method for improving the material surface in terms of mechanical, thermal, chemical and electrical performances. Since titanium compounds generally have a higher melting point and superior anticorrosion properties in comparison with iron, the utilization of the compounds, particularly, titanium carbide (TiC) and titanium nitride (TiN), has increased.

However, the residual stress caused by coating has an effect on the performances of films and occasionally leads to the generation of exfoliations and cracks. Therefore, it is important to examine the residual stress in films. Stress measurement by the X-ray diffraction method is effective for this examination. By means of conventional X-ray stress measurement, i.e., the $\sin^2\psi$ technique, it is possible to measure the average internal stress within the X-ray penetration depth [1,2]. However, the technique is often inapplicable to films coated by chemical vapor deposition (CVD) and physical vapor deposition (PVD), because the technique formulated for the isotropic elastic theory is not applicable to the anisotropic films with the preferred orientations such as <111> and <100>. It is necessary to get rid of the inconsistency for the X-ray stress measurement. In recent years, X-ray stress measurements for films with [001], [111] and [110] fiber textures have been reported by Hanabusa et al. [3] and others [4-6].

In this study, the X-ray stress measurement for <110>-oriented materials was formulated in terms of anisotropic elastic theory. The improvements were mainly the introduction of the crystallite orientation distribution and the X-ray stress determination for the nonlinear relation between measured strain and $\sin^2\psi$, where ψ was the angle between the normals to the diffraction plane and the specimen surface. Moreover, the stress and lattice constant of TiC films were determined by the X-ray stress measurement, and the stress determination was discussed based on the loading experiments.

2. X-RAY STRESS ANALYSIS OF <110>-ORIENTED FILMS

2.1. The X-ray Stress-Strain Relation of Single Cubic Crystal

The crystal system (C) is defined as a Cartesian coordinate system so that the three axes, C_1, C_2 and C_3, correspond to the crystal orientations [100], [010] and [001] in single cubic crystal, respectively. As shown in Fig. 1, the intermediate system (I) is formed as the coordinate system with the I_3 axis along the [110] direction from the C system by the coordinate transformation matrix

$$\alpha_{ij}=\begin{pmatrix} 0 & 0 & -1 \\ -\frac{1}{\sqrt{2}} & \frac{1}{\sqrt{2}} & 0 \\ \frac{1}{\sqrt{2}} & \frac{1}{\sqrt{2}} & 0 \end{pmatrix}. \qquad (1)$$

Rotating the I system about the I_3 axis, the new system is equivalent to the sample coordinate system (S) with which the S_1 and S_3 axes correspond to the longitudinal direction and normal direction of the specimen surface, respectively, as shown in Fig. 2. The coordinate transformation matrix is expressed by

$$\beta_{ij}=\begin{pmatrix} \cos\gamma & \sin\gamma & 0 \\ -\sin\gamma & \cos\gamma & 0 \\ 0 & 0 & 1 \end{pmatrix}, \qquad (2)$$

where γ is the rotation angle from the I to S system.

The laboratory coordinate system (L) is defined so

Received April 4, 2000
Accepted October 28, 2000
Original paper in Japanese was published in Journal of the Society of Materials Science, Japan, Vol. 46, No. 7 (1997) pp. 750-755.

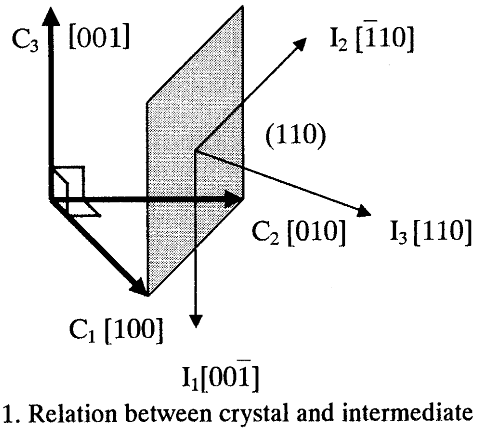

Fig. 1. Relation between crystal and intermediate coordinate systems.

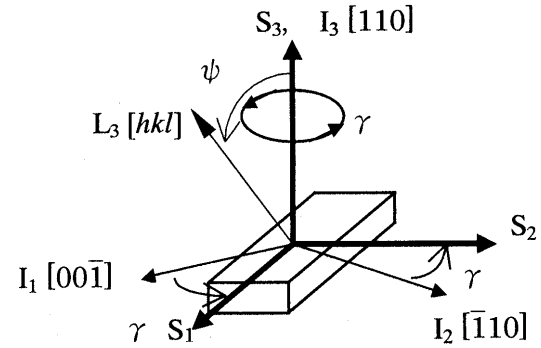

Fig. 2. Relation between intermediate and specimen systems (ϕ=0).

that the L_3 axis is normal to the diffraction plane (*hkl*) by the coordinate transformation matrix ω_{ij} with rotation angles (ϕ,ψ).

$$\omega_{ij}=\begin{pmatrix}\cos\phi\cos\psi & \sin\phi\cos\psi & -\sin\psi\\ -\sin\phi & \cos\phi & 0\\ \cos\phi\sin\psi & \sin\phi\sin\psi & \cos\psi\end{pmatrix} \qquad (3)$$

The elastic compliance S_{ijkl} in the S system is obtained by the coordinate transformation

$$S_{ijkl}=\pi_{ia}\pi_{jb}\pi_{kc}\pi_{kd}S^{C}{}_{abcd}\,, \qquad (4)$$

where $S^C{}_{ijkl}$ is the elastic compliance of the C system and π_{ij} is the transformation matrix from the C to S system, as shown in Fig. 3. Moreover, averaging the elastic compliance S about the S_3 axis, the macroscopic elastic compliance $\langle S\rangle$ of [110]-oriented films is obtained.

$$\langle S\rangle\equiv\frac{\int_0^{2\pi}f(\gamma)S(\gamma)d\gamma}{\int_0^{2\pi}f(\gamma)d\gamma}\,, \qquad (5)$$

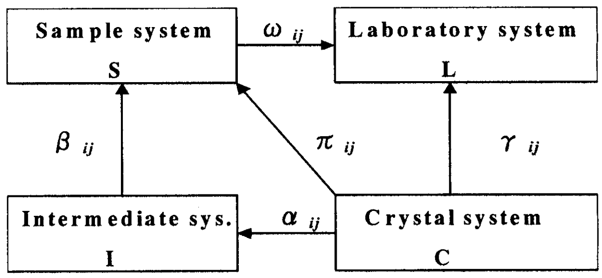

Fig. 3. Definitions of coordinate transformation tensors.

where the weight function $f(\gamma)$ is rated as the contribution of each crystallite orientation and the averaging is denoted by angle brackets.

Substituting the following transformation rules:

$$\varepsilon^{L}{}_{ij}=\gamma_{ik}\gamma_{jl}\varepsilon^{C}{}_{kl}\,,\sigma^{C}{}_{ij}=\pi_{ki}\pi_{lj}\sigma^{S}{}_{kl}\,,\ \gamma_{ij}\equiv\omega_{ia}\pi_{aj}\,, \qquad (6)$$

into the stress-strain relation $\varepsilon^{C}{}_{ij}=S^{C}{}_{ijkl}\sigma^{C}{}_{kl}$ in the C system, the relation between the stress $\sigma^{S}{}_{ij}$ in the S system and the strain $\varepsilon^{L}{}_{33}$ in the L system is given as

$$\varepsilon^{L}{}_{33}=S^{X}{}_{33ij}\sigma^{S}{}_{ij}\,, \qquad (7)$$

where $S^X{}_{33ij}$ is defined by

$$S^{X}{}_{33ij}\equiv\gamma_{3a}\gamma_{3b}S^{C}{}_{abcd}\pi_{ic}\pi_{jd}=\omega_{3a}\omega_{3b}S_{abij}\,, \qquad (8)$$

$$\begin{aligned}S^{X}{}_{33ij}&=(S_{11ij}\cos^2\phi+S_{22ij}\sin^2\phi\\&\quad+S_{12ij}\sin 2\phi-S_{33ij})\sin^2\psi+S_{33ij}\\&\quad+(S_{13ij}\cos\phi+S_{23ij}\sin\phi)\sin 2\psi.\end{aligned} \qquad (9)$$

For the principal stress state and ϕ=0, there is no $\sin 2\psi$ term in the X-ray stress-strain relation as follows:

$$\begin{aligned}\varepsilon^{L}{}_{33}&=[(S_{1111}-S_{1133})\sigma^{S}{}_{1}+(S_{1122}-S_{2233})\sigma^{S}{}_{2}\\&\quad+(S_{1133}-S_{2233})\sigma^{S}{}_{3}]\sin^2\psi\\&\quad+S_{1133}\sigma^{S}{}_{1}+S_{2233}\sigma^{S}{}_{2}+S_{3333}\sigma^{S}{}_{3}.\end{aligned} \qquad (10)$$

However, Eq. (10) has nonlinearity in the $\sin^2\psi$ diagram because the elastic compliance in the S system is a function of γ.

The X-ray stress-strain relations have been calculated for the [111] and [100] fiber textures by Hanabusa et al. [3] and others [4-6].

$$\frac{\varepsilon^{L}{}_{33}}{\sigma^{S}}=\begin{cases}\dfrac{2}{3}S^{C}{}_{0}+2S^{C}{}_{12}+S^{C}{}_{44}\sin^2\psi & \text{for}\,[111]\\ 2S^{C}{}_{12}+\left(S^{C}{}_{11}-S^{C}{}_{12}\right)\sin^2\psi & \text{for}\,[100],\end{cases} \qquad (11)$$

$$S^{C}{}_{0}\equiv S^{C}{}_{11}-S^{C}{}_{12}-\frac{1}{2}S^{C}{}_{44}\,, \qquad (12)$$

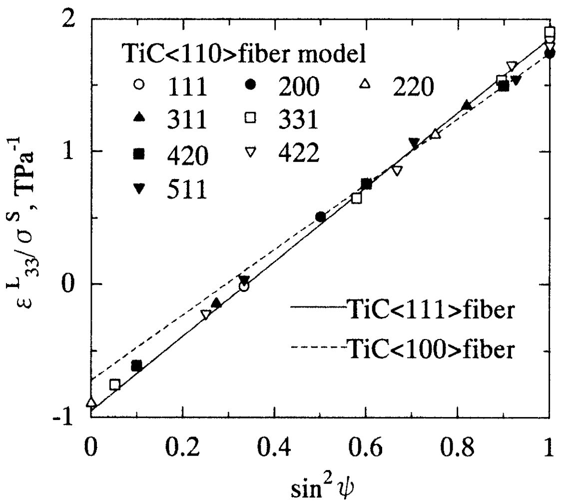

(a) TiC fiber model with S^{C}_{0}=-0.35TPa^{-1}.

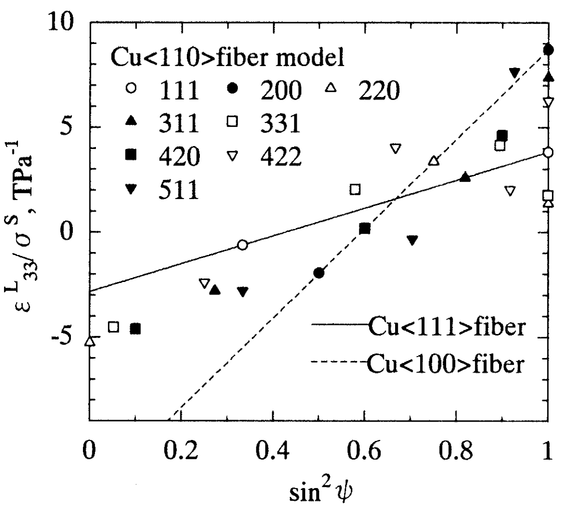

(b) Cu fiber model with S^{C}_{0}=14.7TPa^{-1}.

Fig. 4. Lattice strain distribution for <110>-oriented model of TiC and Cu in biaxial stress state.

where S^{C}_{11}, S^{C}_{12}, S^{C}_{44} are the three independent components of the elastic compliance for single cubic crystal. As shown by each straight line in Fig. 4, Eq. (11) has linearity in the $\sin^2\psi$ diagram.

2.2. The X-ray Stress-Strain Relations of Polycrystalline Films

Although macroscopic mechanical behaviors of oriented film are invariable for rotation around the S_3 axis, not all crystallites contribute to the X-ray diffraction; only those crystallites that satisfy the diffraction condition can be measured. Therefore, it is necessary to average the lattice strain by the weight function from the effective crystallite distribution of the X-ray diffraction. The averaged lattice strain $\langle \varepsilon^{L}_{33} \rangle$ is obtained from Eq. (10) as follows:

$$\frac{\langle \varepsilon^{L}_{33} \rangle}{\sigma^{S}} = \frac{1}{2}\left(S^{C}_{0}\langle \cos^2\gamma \rangle + S^{C}_{44}\right)\sin^2\psi + \frac{1}{2}S^{C}_{0} + 2S^{C}_{12} \ , \tag{13}$$

$$\frac{\langle \varepsilon^{L}_{33} \rangle}{\sigma^{S}_{1}} = [S^{C}_{0}\langle \cos^2\gamma(1-\frac{3}{2}\sin^2\gamma) \rangle + \frac{1}{2}S^{C}_{44}]\sin^2\psi + \frac{1}{2}S^{C}_{0}\langle \sin^2\gamma \rangle + S^{C}_{12} \ , \tag{14}$$

where the Reuss model in which the stress is assumed to be constant [7]. Biaxial and uniaxial stress states are assumed for Eqs. (13) and (14), respectively.

Measuring the diffraction plane (*hkl*) of oriented films, the $\boldsymbol{S}_1$ vector along the S_1 axis and the particular angle γ_P for diffracted crystallites are uniquely determined because the L_3 and S_3 axes are given by [*hkl*] and [110] in the C system, respectively.

$$\boldsymbol{S}_1 = \left(h-k,\ -(h-k),\ 2l\right), \tag{14}$$

$$\gamma_P = \arctan\left(\frac{1}{\sqrt{2}}\cdot\frac{k-h}{l}\right). \tag{15}$$

2.3. X-ray Stress Analysis for <110>-Oriented TiC Films

The values of $\varepsilon^{L}_{33}/\sigma^{S}$ were calculated for TiC 420 diffraction with (S^{C}_{11}, S^{C}_{12}, S^{C}_{44})=(2.10, -0.36, 5.61) [1/TPa] [8] by Eq. (13). Table 1 presents the numerical results. In the calculation, the Dirac delta function was applied for the crystallite orientation distribution $f(\gamma)$, because only the crystallites with the particular angle γ_P can contribute to the diffraction. [*abc*] and *E* are the direction and Young's modulus along the S_1 axis for measured crystallites, respectively. For available X-ray diffraction planes, Fig. 4 (a) also shows the numerical results of Eq. (13) in relation to $\sin^2\psi$. These values are slightly different from the straight line in Fig. 4 (a). For comparison with TiC, the numerical results for copper with (S^{C}_{11}, S^{C}_{12}, S^{C}_{44})=(15.0, -6.3, 13.3)[1/TPa] [8] are shown in Fig. 4 (b). It is evident that the larger the S^{C}_{0} of

Table 1. Numerical values of $\varepsilon^{L}_{33}/\sigma^{S}$ and Young moduli from the measured planes for 420 for <110>-oriented TiC film in biaxial stress state (ψ < 60 deg).

hkl	ψ, deg	$\sin^2\psi$	γ_P, deg	$\varepsilon^{L}_{33}/\sigma^{S}$, 1/TPa	S_1 [*abc*]	S_{11}, 1/TPa	*E*, GPa
420	18.4	0.10	-90	-0.612	$[1\bar{1}0]$	2.27	440.0
240			90		$[\bar{1}10]$		
402	50.8	0.60	-125	0.756	$[1\bar{1}1]$	2.33	429.2
042			125		$[\bar{1}11]$		
$40\bar{2}$			-54.7		$[1\bar{1}\bar{1}]$		
$04\bar{2}$			54.7		$[\bar{1}1\bar{1}]$		

the elastic anisotropy, the greater the nonlinearity of <110>-oriented materials. Generally, the conventional $\sin^2\psi$ technique which uses the linearity is inapplicable to <110>-oriented materials. Therefore, it is necessary to determine the X-ray stress by a different calculation without using the linearity.

(1) Measurement for the diffraction plane $\{hkl\}$

Since the lattice strain is obtained from

$$\varepsilon^{L}{}_{33} = \frac{d - d_0}{d_0}, \tag{16}$$

Eq. (13) may be expressed as

$$d = d_0\left(S\,\sigma^{S} + 1\right), \tag{17}$$

where S represents the right-hand side of Eq. (13) and d and d_0 are the stressed and unstressed lattice spacings, respectively. Provided that the elastic constants of the single crystal are known, S only has the parameter (hkl). Hereby, if the diffraction plane can be measured in different ψ angles as (ψ_1, d_1) and (ψ_2, d_2), Eq. (17) for two measured values (d_1, S_1), (d_2, S_2) becomes the simultaneous equations of (σ^S, d_0). Namely,

$$\sigma^{S} = \frac{d_2 - d_1}{d_1S_2 - d_2S_1}, \quad d_0 = \frac{d_1S_2 - d_2S_1}{S_2 - S_1}. \tag{18}$$

(2) Measurement for different diffraction planes

The X-ray stress and lattice constant a_0, instead of d_0, can be determined from Eq. (17) by the least-squares method for nonlinear parameters [9]. The matrix equation is obtained by the method for the measured values (a_i, S_i) as follows

$$\begin{pmatrix} \sum_i \left(S_i\sigma^S + 1\right)^2 & a_0\sum_i S_i\left(S_i\sigma^S + 1\right) \\ a_0\sum_i S_i\left(S_i\sigma^S + 1\right) & \sum_i \left(a_0S_i\right)^2 \end{pmatrix}\begin{pmatrix} \delta a_0 \\ \delta\sigma^S \end{pmatrix} = \begin{pmatrix} -\sum_i \left(S_i\sigma^S + 1\right)R_i \\ -\sum_i a_0S_iR_i \end{pmatrix}, \tag{19}$$

where $R = a_i^0 - a_i$ and a_i^0 is an estimated value for the measurement of the lattice constant. Solving the matrix equation for $(\delta a_0, \delta\sigma^S)$ by the iterative method, the stress and lattice constant can be determined from

$$a_0 = a_0{}^0 + \delta a_0, \quad \sigma^S = \sigma^{S0} + \delta\sigma^S, \tag{20}$$

where $a_0{}^0$ and σ^{S0} are initial estimates of the lattice constant and stress, respectively.

3. EXPERIMENTS

3.1. Specimen

The specimen is coated with TiC film on a piece of high-speed cutting tool (JIS: SKH51) by CVD. CVD coating was carried out four times with 3.6, 3.5, 3.7 and 3.7 μm thickness. The thickness of the film is approximately 14.5 μm on the 50-mm-long, 10-mm-wide and 5.7-mm-thick substrate. Figure 5 shows the relation between the ψ angle and the X-ray diffraction intensity. It is understood that there is a preferred orientation with <110>.

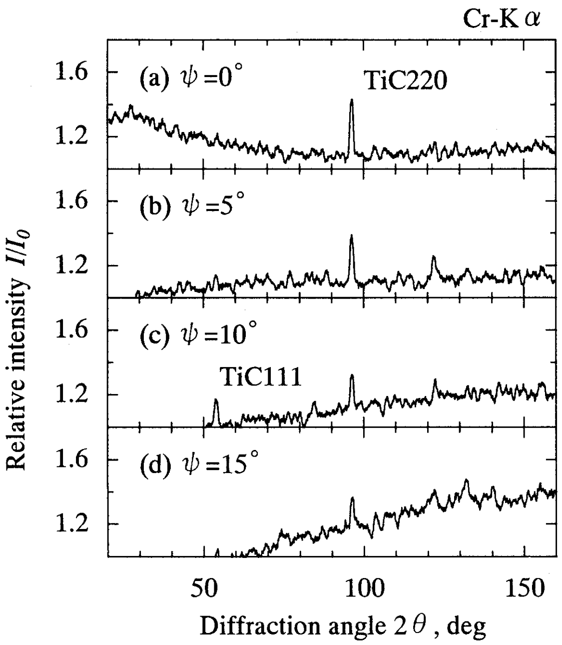

Fig. 5. Diffraction pattern of TiC film.

3.2. X-ray Stress Measurement

An X-ray instrument with parallel beam optics was used. The diffraction profiles of TiC 420 by CoKα X-rays were measured. These measurement conditions are listed in Table 2. The diffraction intensity and diffraction angle 2θ were measured around ψ=18 and 51 deg for the TiC420 diffraction, because the angles are determined by the crystallographic relation, as shown in Table 1. Then, two angles of (ψ_1, ψ_2) in the intensity peak were calculated by parabola approximation, and $(2\theta_1, 2\theta_2)$ at these peak positions were determined by the

Table 2. Condition of X-ray stress measurement.

X-ray tube	CoKα
Diffraction planes	TiC420
Diffraction angle	135.29deg
Tube voltage, current	30kV, 10mA
Step width for peak and BG area	0.2 and 1.0deg
Peak determination	Half value method
Fixed time	10s
Scanning method	Fixed ψ method

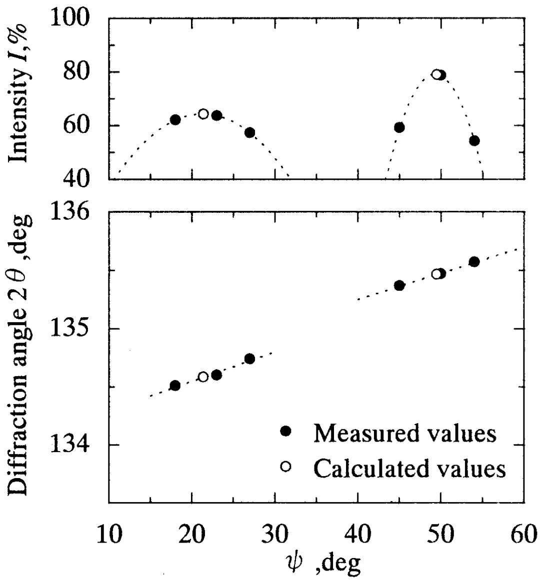

Fig. 6. Diffraction angle and lattice strain distribution of TiC420 measurement.

linear approximation shown in Fig. 6. Finally, the X-ray stress was determined by the following equation obtained from the Bragg condition $2d\sin\theta = n\lambda$ and Eq. (18):

$$\sigma^S = -\frac{\sin\theta_2 - \sin\theta_1}{S_2\sin\theta_2 - S_1\sin\theta_1}. \qquad (21)$$

3.3. Comparison between X-ray Stress and Applied Stress

The measured stress σ^S by Eq. (21) was compared with the applied stress σ^A by a small four-point bending jig in order to verify the effectiveness of the X-ray stress measurement. The applied strain ε^A was measured using a strain gage on the substrate, and the applied stress was calculated as the product of the mechanical elastic costant and the applied strain. The macroscopic elastic constant E^A=444.26 GPa was calculated by Eq. (5). Then, the X-ray strain was calculated by Hooke's law $\varepsilon^S_{11} = S_{11}\sigma^S_1$ in the S system. For two specific angles (ψ_1, ψ_2)=(18.4, 50.8) deg, these values of S_{11} along the S_1 axes were estimated as (2.27, 2.33)/TPa, as shown in Table 1.

4. RESULTS AND DISCUSSION

4.1. Residual Stress Value of TiC Film

The X-ray stress was determined by Eq. (21) for TiC 420 diffraction from the measured values of (ψ_1, $2\theta_1$; ψ_2, $2\theta_2$)=(21.4, 134.6; 49.5, 135.5) deg. Then, the lattice constant a_0=0.4335nm and diffraction angle $2\theta_0$= 134.97 deg were calculated by Eq. (18). Table 3 presents the X-ray stress values by the present method and those obtained by the isotropic Reuss model. In the isotropic Reuss model, the stress is determined by

Table 3. Stress values and $2\theta_0$ of each model for TiC420.

	Stress σ^S, GPa	Diffraction angle, $2\theta_0$, deg
Present method	-2.33	134.97
Isotropic Reuss model	-2.73	---
TiC powder	---	135.00

$$\sigma^S = \left[S^C{}_0(1-3\Gamma) + \frac{1}{2}S^C{}_{44}\right]^{-1} \cdot \frac{\partial \varepsilon^L{}_{33}}{\partial \sin^2\psi}, \qquad (22)$$

$$\Gamma = \frac{h^2k^2 + k^2l^2 + l^2h^2}{\left(h^2+k^2+l^2\right)^2}, \qquad (23)$$

where the unstressed diffraction angle $2\theta_0$ was measured from the TiC powder.

High compressive stresses were measured in the film and the absolute value of stress was smaller for the present method than for the isotropic Reuss model.

4.2. Applied Stress Value

The experiments were conducted under the condition of the applied strain values 0, 0.50×10^{-3} and 1.0×10^{-3}. Table 4 and Fig. 7 show the results and the relation be-

Table 4. Applied and X-ray strain and stress values.

Applied strain $\varepsilon^A/10^{-3}$	Applied stress σ^A, MPa	X-ray stress σ^X, GPa	X-ray strain $\varepsilon^X/10^{-3}$ along S_1 for ψ_1, ψ_2
0	0	-2.33	-5.30, -5.44
0.50	222.1	-2.08	-4.73, -4.85
1.0	444.3	-1.79	-4.06, -4.16

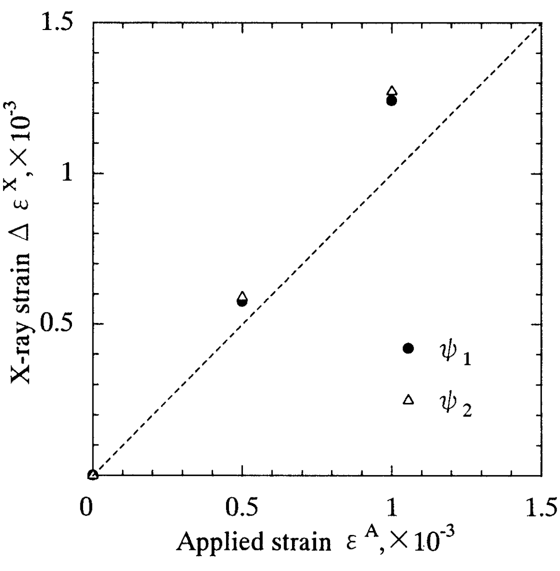

Fig. 7. Difference between applied and X-ray strain for TiC420 diffraction.

tween the applied strain and the reduced X-ray strain $\Delta \varepsilon^X$: the difference between the applied and unapplied stress states. The reduced strain was represented in order to lower the influence of residual stress. There is a difference between the applied strain and the reduced X-ray strain. It is evident that the X-ray strain is not necessarily equivalent to the macrostrain. Since the measured crystallites in the specimen only satisfy the X-ray diffraction condition, the number of measured crystallites is far less than the number of crystallites contributing to the applied strain. Provided that all crystallites are measurable by X-ray diffraction, the averaged X-ray strain may approximate the applied strain. As a series of experiments, it is necessary to verify the X-ray stress measurement for <110>-oriented films by a loading test, inclusive of the measurement of the mechanical elastic constants, and to take the imperfectly oriented films and the interaction among crystallites into consideration.

5. CONCLUSIONS

(1) The X-ray stress measurement for <110>-oriented films was formulated. The X-ray stress-strain relation revealed nonlinearity in the relation between the lattice strain and the $\sin^2\psi$ for the dependence of diffraction planes.
(2) If two kinds of diffraction planes, for instance 420 and 402 planes, are measurable, then X-ray stress determination without the unstressed lattice spacing was manifested for <110>-oriented materials. Moreover, for the measured data of plural diffraction planes, the X-ray stress determination was proposed by the least-squares method for nonlinear parameters.
(3) The stress determination was applied to the present TiC film coated by CVD since the specimen had a <110> preferred orientation normal to the specimen surface. As a result, compressive stress could be measured in the film.
(4) It was possible to calculate the elastic constant of measured crystallites and the strain value by the X-ray diffraction method. It was evident that the values were not always equal to macroscopic values.

Acknowledgements —The authors would like to thank Dr. K. Okazaki and President K. Fujita of Fujita Giken Co., Ltd., for providing the TiC specimens.

REFERENCES

1. I.C. Noyan and J. B. Cohen, Residual Stress, Springer-Verlag, New York (1987).
2. The Method of X-ray Stress Measurement (ed. by Soc. Mater. Sci., Japan), Yoken-do (1981) (in Japanese).
3. T. Hanabusa, K. Tominaga and H. Fujiwara, J. Soc. Mater. Sci., Japan, **42** (1993) 90 (in Japanese).
4. K. Tanaka and K. Ishihara, Trans. JSME, Ser. A, **61** (1995) 1971 (in Japanese).
5. M. Zaouali, J. L. Lebrun and P. Gergud, Surf. Coat. Technol., **50** (1991) 5.
6. B. M. Clemens and J. A. Bain, MRS Bulletin, **17** (1992) 46.
7. A. Reuss, Z. ang. Math. Mech., **9** (1929) 49.
8. Landolt-Börnstein (Group III-Vol. II) (ed. by K.-H.Hellwege), Springer-Verlag, New York (1979) p. 30.
9. T. R. MaCalla, Introduction to Numerical Methods & Fortran Programming, John Wiley & Sons, New York (1967).